

RESEARCH

Open Access



hsa-miR-100-5p, an overexpressed miRNA in human ovarian endometriotic stromal cells, promotes invasion through attenuation of SMARCD1 expression

Kanetoshi Takebayashi¹, Kaei Nasu^{1,2*}, Mamiko Okamoto¹, Yoko Aoyagi¹, Tomoko Hirakawa¹ and Hisashi Narahara¹

Abstract

Background: A number of microRNAs are aberrantly expressed in endometriosis and are involved in its pathogenesis. Our previous study demonstrated that has-miR-100-5p expression is enhanced in human endometriotic cyst stromal cells (ECSCs). The present study aimed to elucidate the roles of has-miR-100-5p in the pathogenesis of endometriosis.

Methods: Normal endometrial stromal cells (NESCs) were isolated from normal eutopic endometrium without endometriosis. Using hsa-miR-100-5p-transfected NESCs, we evaluated the effect of hsa-miR-100-5p on the invasiveness of these cells by Transwell invasion assay and in-vitro wound repair assay. We also investigated the downstream signal pathways of hsa-miR-100-5p by microarray analysis and Ingenuity pathways analysis.

Results: hsa-miR-100-5p transfection enhanced the invasion and motility of NESCs. After hsa-miR-100-5p transfection, mRNA expression of SWItch/sucrose non-fermentable-related matrix-associated actin-dependent regulator of chromatin subfamily D member 1 (SMARCD1) was significantly attenuated. Whereas, the expression of matrix metalloproteinase 1 (MMP1) mRNA and active MMP1 protein levels was upregulated.

Conclusion: We found that SMARCD1/MMP-1 is a downstream pathway of hsa-miR-100-5p. hsa-miR-100-5p transfection enhanced the motility of NESCs by inhibiting SMARCD1 expression and MMP1 activation. These findings suggest that enhanced hsa-miR-100-5p expression in endometriosis is involved in promoting the acquisition of endometriosis-specific characteristics during endometriosis development. Our present findings on the roles of hsa-miR-100-5p may thus contribute to understand the epigenetic mechanisms involved in the pathogenesis of endometriosis.

Keywords: Endometriosis, Invasion, Hsa-miR-100-5p, SMARCD1, Matrix metalloproteinase 1

* Correspondence: nasu@oita-u.ac.jp

¹Department of Obstetrics and Gynecology, Faculty of Medicine, Oita University, Idaigaoka 1-1, Hasama-machi, Yufu-shi, Oita 879-5593, Japan

²Division of Obstetrics and Gynecology, Support System for Community Medicine, Faculty of Medicine, Oita University, Oita, Japan



© The Author(s). 2020 **Open Access** This article is licensed under a Creative Commons Attribution 4.0 International License, which permits use, sharing, adaptation, distribution and reproduction in any medium or format, as long as you give appropriate credit to the original author(s) and the source, provide a link to the Creative Commons licence, and indicate if changes were made. The images or other third party material in this article are included in the article's Creative Commons licence, unless indicated otherwise in a credit line to the material. If material is not included in the article's Creative Commons licence and your intended use is not permitted by statutory regulation or exceeds the permitted use, you will need to obtain permission directly from the copyright holder. To view a copy of this licence, visit <http://creativecommons.org/licenses/by/4.0/>. The Creative Commons Public Domain Dedication waiver (<http://creativecommons.org/publicdomain/zero/1.0/>) applies to the data made available in this article, unless otherwise stated in a credit line to the data.

Background

Endometriosis belongs to estrogen-dependent benign tumors and occurs in 6–10% of the women of reproductive age [1]. The microscopic features of endometriotic tissues resemble those of proliferative-phase endometrial tissues [1]; however, molecular studies have revealed a number of differences at the epigenetic, genetic, transcriptional, and posttranscriptional levels [2–5].

To understand the mechanism(s) responsible for the pathogenesis of endometriosis, we have previously investigated microRNA (miRNA) expression levels in endometriosis [4–7]. Our previous microarray study detected a repertoire of aberrantly expressed miRNAs in endometriosis [4]. Of these aberrantly expressed miRNAs, we demonstrated that upregulation of hsa-miR-210 [5] and downregulation of hsa-miR-196b [4] and hsa-miR-503 [6] contribute to the pathogenesis of endometriosis. Hsa-miR-210 induced the cell proliferation and vascular endothelial cell growth factor (VEGF) production of human normal endometrial stromal cells (NESC) and inhibited apoptosis of these cells [5]. Whereas, hsa-miR-196b induced the apoptosis of human endometriotic cyst stromal cells (ECSCs) and inhibited the proliferation of these cells [4]. hsa-miR-503 also induced the cell-cycle arrest at G0/G1 phase and apoptosis and inhibited the cell proliferation, VEGF production, and contractility of ECSCs [6].

SWI/SNF-related matrix-associated actin-dependent regulator of chromatin subfamily D member 1 (SMARCD1) belongs to the SWI/SNF chromatin remodeling complex family of proteins which regulate the target gene transcription by altering the local chromatin structure around those genes [8, 9]. SMARCD1 is often involved in somatic rearrangement in tumorigenesis [10]. The chromatin remodeling activity of SMARCD1 is essential for tumor suppression [11, 12]. We speculated that SMARCD1 suppression may induce tumorigenesis in endometriosis.

Matrix metalloproteinase 1 (MMP1) is a key enzyme that promotes the breakdown of extracellular matrix during physiological and pathological processes such as embryonic development, reproduction, and tissue remodeling, as well as tumor invasion and metastasis. MMP-1 is the most ubiquitously expressed interstitial collagenase that cleaves the interstitial collagen, types I, II, and III [13]. MMP1 is overexpressed in endometriotic tissues, suggesting its involvement in the pathogenesis of endometriosis [14].

In the present study, we evaluated the role of hsa-miR-100-5p, a miRNA that is upregulated in ECSCs, regarding the pathogenesis of endometriosis [4]. Using hsa-miR-100-5p-transfected NESC, we assessed the effect of hsa-miR-100-5p on the invasiveness of these cells and the expression of SMARCD1 and MMP1, which are downstream targets of hsa-miR-100-5p, in these cells.

Methods

Human NESC and ECSC isolation procedures and cell culture conditions

Normal endometrial tissues were collected at the time of hysterectomies from patients with subserous or intramural leiomyoma who had regular menstrual cycle and had no evidence of endometriosis ($n = 13$, age 31–53 yrs.), as described previously [15]. Whereas, ovarian endometrioma tissues were obtained at the time of surgical treatment from patients with regular menstrual cycles ($n = 6$, age 22–42 yrs.), as described before [6, 7, 15]. None of the patients had received the hormonal treatments for at least 2 years prior to the surgery. Pathological examination and/or menstrual records confirmed that all the specimens were in the mid-to-late proliferative phases. This study was approved by the Institutional Review Board (IRB) of the Faculty of Medicine, Oita University (registration number: P-16-01), and written informed consent was obtained from all the patients.

ECSCs and NESC were isolated from ovarian endometrioma and normal endometrial tissues, respectively, by enzymatic digestion, and cultured in Dulbecco's modified Eagle's medium (DMEM) supplemented with 100 IU/ml of penicillin (Gibco-BRL, Gaithersburg, MD, USA), 50 mg/ml of streptomycin (Gibco-BRL), and 10% charcoal-stripped heat-inactivated fetal bovine serum (FBS) (Gibco-BRL) at 37 °C in 5% CO₂ in air, as described previously [6, 7, 15]. This culture condition is free of ovarian steroid hormones. Each experiment was performed in triplicate and was repeated at least three times with cells isolated from separate patients.

Quantitative reverse transcription-polymerase chain reaction (RT-PCR) for hsa-miR-100-5p

In our previous study, using a miRNA microarray technique, we demonstrated that hsa-miR-100-5p was upregulated in ECSCs [4]. For the validation of the microarray data, we performed quantitative RT-PCR with NESC ($n = 6$) and ECSCs ($n = 6$) as described previously [4–6]. hsa-miR-100-5p-specific (Assay ID: 000437, Applied Biosystems, Carlsbad, CA, USA) or endogenous control (RNU44)-specific (Assay ID: 001094, Applied Biosystems) reverse primers were used. The expression levels of hsa-miR-100-5p were normalized to those of RNU44, calculated by the $\Delta\Delta CT$ method, and were presented as the relative expression in ECSCs compared to that in NESC.

Transfection of miRNA precursors and small interfering RNAs (siRNAs)

Precursor hsa-miR-100-5p (pre-miR miRNA precursor-hsa-miR-100-5p, Ambion, Austin, TX, USA), negative control precursor miRNA (pre-miR miRNA precursor-negative control #1, Ambion), SMARCD1 silencer pre-designed siRNA (AM16708, Ambion) or Silencer® select

negative control #1 siRNA (Ambion) were transfected into NESCs using Lipofectamine RNAiMAX (Invitrogen, Carlsbad, CA, USA) and the reverse transfection method, as described before [4–6].

Gene expression microarray

Forty-eight hours after transfection, total RNA was extracted from cultured NESCs transfected with precursor hsa-miR-100-5p ($n = 4$) and NESCs transfected with negative control precursor miRNA ($n = 4$) using an RNeasy Mini kit (Qiagen, Valencia, CA, USA) and subjected to gene expression microarray analyses with a commercially available human mRNA microarray (G4851A, SurePrint G3 Human Gene Expression Microarray 8x60K v2, Agilent Technologies, Santa Clara, CA, USA), as described previously [5]. To identify the upregulated and downregulated genes, the Z-scores and ratios (non-log scaled fold-change) from the normalized signal intensities of each probe were calculated to compare between NESCs transfected with precursor hsa-miR-100-5p and NESCs transfected with negative control precursor miRNA [5]. We established the following criteria for the regulated genes: at least 3 out of 4 samples has Z-score ≥ 2.0 and ratio ≥ 2.0 -fold for upregulated genes, and Z-score ≤ -2.0 and ratio ≤ 0.5 for downregulated genes. All the gene expression microarray data are available at the Gene Expression Omnibus through the NCBI under Accession No. GSE139954 (<https://www.ncbi.nlm.nih.gov/geo/query/acc.cgi?acc=GSE139954>).

miRNA target prediction and pathways analysis

To elucidate the downstream target genes and signal pathways of hsa-miR-100-5p, datasets representing the genes with an altered expression profile derived from the microarray analyses were analyzed by the Ingenuity pathways analysis (IPA) software (Ingenuity Systems, Redwood City, CA, USA) with the IPA knowledgebase (IPA Summer Release 2015). Thereafter, predicted targets of hsa-miR-100-5p were confirmed by online public databases including miRDB (<http://mirdb.org/miRDB/>), TargetScanHuman (<http://www.targetscan.org/>, Release 7.0), PicTar (<http://pictar.mdc-berlin.de/>), and microRNA.org (<http://www.microrna.org/microrna/getGeneForm.do>).

Transwell invasion assay

The invasive properties of hsa-miR-100-5p-transfected NESCs were evaluated by Transwell invasion assay, as described previously [16, 17]. NESCs after miRNA transfection (2×10^5 cells) were cultured in DMEM supplemented with 10% charcoal-stripped heat-inactivated FBS on the growth factor-reduced Matrigel-coated Transwell inserts with 8- μ m pores (Corning Inc., New York, NY, USA). After 48 h, the membranes were fixed with 100%

methanol, and the number of cells appearing on the undersurface of the polycarbonate membranes after Giemsa staining was scored visually at $\times 200$ magnification using a light microscope.

The data from triplicate samples were calculated and presented as the percent values obtained for the NESCs transfected with precursor hsa-miR-100-5p relative to those transfected with the negative control precursor miRNA.

In vitro wound repair assay

Cell motility was also determined by an in vitro wound repair assay, as described previously [16, 17]. NESCs grown to confluence in 6-well plates (Corning Inc.) were challenged overnight with serum-free medium and then transfected with the miRNA precursor. The monolayer was wounded using a cell scraper and the plates were incubated in DMEM plus 0.1% BSA for 48 h. The cells were then fixed with 3% paraformaldehyde and stained with Giemsa solution. Areas with lesions were photographed, and wound repair was assessed by calculating the repaired area in square micrometers between the lesion edges at 0 h and 48 h using the public domain software Image J 1.44 developed at the U.S. National Institutes of Health (Bethesda, MD, USA).

The data from triplicate samples were calculated and presented as the percent values obtained for the NESCs transfected with precursor hsa-miR-100-5p relative to those transfected with the negative control precursor miRNA.

RT-PCR for mRNA expression

The effects of hsa-miR-100-5p on the expression levels of possible downstream target genes were evaluated in ECSCs by quantitative RT-PCR, as described [4–6]. *SMARCD1* and *MMP1* were selected as candidate genes because *SMARCD1* was confirmed to be the predicted target of hsa-miR-100-5p in the online public database, TargetScanHuman (<http://www.targetscan.org/>, Release 7.2). *MMP1* is known to be the downstream target of *SMARCD1* [18] and promotes cell motility (Fig. 1).

In brief, 48 h after miRNA transfection, total RNA from miRNA-transfected NESCs was extracted as described above and subjected to quantitative RT-PCR with the following specific primers (all from Applied Biosystems): *SMARCD1* (Assay ID: Hs00161980_m1), *MMP1* (Assay ID: Hs00899658_m1), or glyceraldehyde 3-phosphate dehydrogenase (*GAPDH*) (Assay ID: Hs02758991_g1). The expression levels of candidate mRNAs relative to those of *GAPDH* mRNA were calculated using a calibration curve. The data were calculated from triplicate samples and are presented as percent values obtained for NESCs after hsa-miR-100-5p

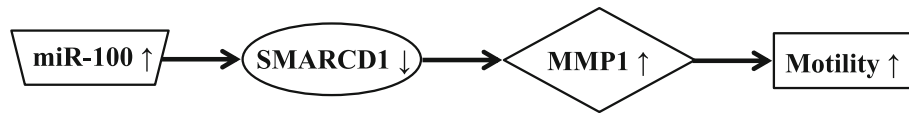


Fig. 1 Downstream signaling pathway of hsa-miR-100-5p in NESC. A gene expression microarray and pathway analyses of hsa-miR-100-5p-transfected NESC revealed that hsa-miR-100-5p upregulated the motility of NESC by direct inhibition of SMARCD1 expression followed by MMP1 activation. SMARCD1, SWItch/sucrose non-fermentable-related matrix-associated actin-dependent regulator of chromatin subfamily D member 1; MMP1, matrix metalloproteinase 1; NESC, normal endometrial stromal cells

transfection relative to those transfected with the negative control precursor miRNA.

ELISA for active MMP1

Culture media of miRNA-transfected NESC were collected 48 h after miRNA transfection and subjected to Human Active MMP-1 Fluorescent Assay (F1M00, R&D Systems, Minneapolis, MN, USA), according to the manufacturer's instructions. The data from triplicate samples were calculated and presented as the percent values obtained for NESC transfected with precursor hsa-miR-100-5p relative to those transfected with the negative control precursor miRNA.

Statistical analysis

All data were obtained from triplicate samples and are presented as percent values relative to the corresponding controls in the form of mean \pm SD. Data were appropriately analyzed by the Student's *t*-test using the Statistical Package for Social Science software (IBM SPSS statistics 24; IBM, Armonk, NY, USA). *P*-values < 0.05 were considered statistically significant.

Results

Expression of hsa-miR-100-5p

To validate the miRNA microarray data [4], we evaluated the hsa-miR-100-5p expression levels in NESC and ECSC using quantitative RT-PCR. As shown in Fig. 2, the relative hsa-miR-100-5p levels in the ECSC were significantly higher than those in the NESC ($p < 0.0005$). Thus, the results of quantitative RT-PCR for hsa-miR-100-5p expression were consistent with our previous miRNA microarray data [4]. Age of the patients did not affect the expression of hsa-miR-100-5p (data not shown).

As shown in Fig. 3a, mature hsa-miR-100-5p expression in NESC was significantly induced by hsa-miR-100-5p precursor transfection ($p < 0.05$). We thus considered this experimental model as appropriate for hsa-miR-100-5p functional analyses.

Identification of hsa-miR-100-5p-regulated genes and predicted pathways in NESC

As shown in Table 1, gene expression microarray analyses detected 33 upregulated and 27 downregulated

mRNAs using the criteria described above. Using the online public databases, we focused on SMARCD1 involved in the pathogenesis of endometriosis. The IPA software then identified MMP1 as a downstream target of SMARCD1 (Fig. 1). Regarding the known function of MMP1, we evaluated the cell motility of NESC using the following experiments.

Modulation of downstream target molecule expression by hsa-miR-100-5p transfection

To investigate the underlying mechanisms of hsa-miR-100-5p functions, we investigated the expression levels of SMARCD1 and MMP1. As shown in Fig. 3b, SMARCD1 mRNA expression was significantly attenuated by hsa-miR-100-5p transfection ($p < 0.05$). In contrast, as shown in Fig. 3c and d, the expression levels of MMP1 mRNA, and active MMP1 protein were upregulated by hsa-miR-100-5p transfection ($p < 0.0005$ and $p < 0.0005$, respectively).

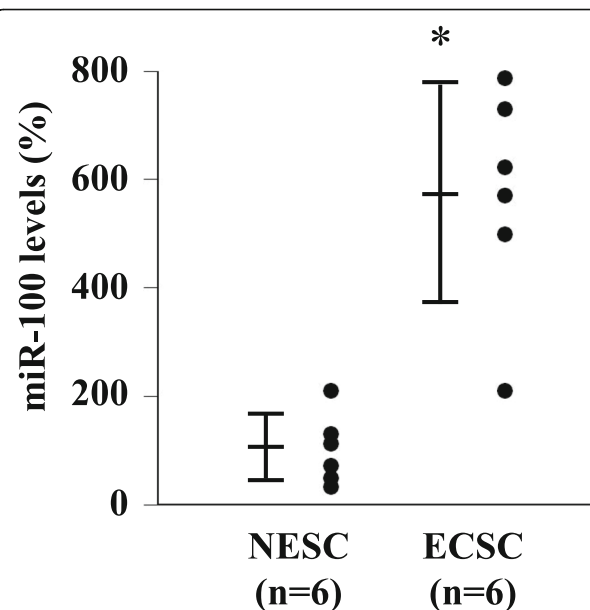


Fig. 2 hsa-miR-100-5p expression in NESC and ECSC. The relative hsa-miR-100-5p levels in ECSC ($n = 6$) were significantly higher than those in the NESC ($n = 6$). * $p < 0.0005$ vs. NESC (Student's *t*-test). Data are shown as the mean \pm SD. ECSC, endometriotic cyst stromal cells; NESC, normal endometrial stromal cells

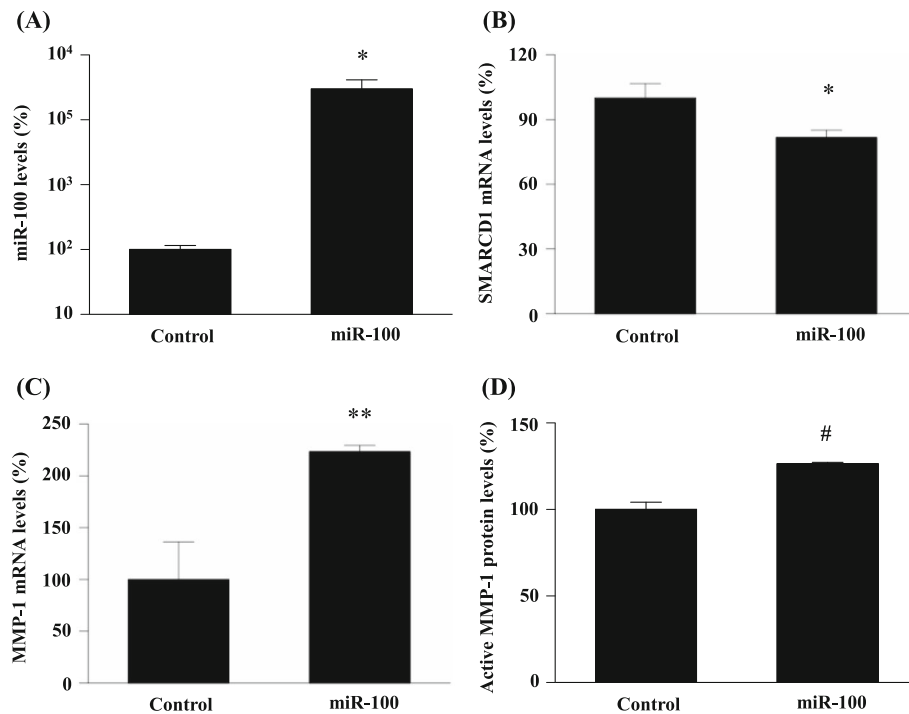


Fig. 3 Effects of hsa-miR-100-5p transfection on the downstream target molecule expression in NESC. **(a)** hsa-miR-100-5p expression after precursor miRNA transfection. Note that the vertical axis is expressed as a logarithmic scale. **(b)** *SMARCD1* mRNA expression. **(c)** *MMP1* mRNA expression. **(d)** Active MMP1 protein expression. * $p < 0.05$, ** $p < 0.005$, # $p < 0.0005$ vs. controls (Student's *t*-test). MMP1, matrix metalloproteinase 1; NESC, normal endometrial stromal cells; *SMARCD1*, SWItch/sucrose non-fermentable-related matrix-associated actin-dependent regulator of chromatin subfamily D member 1

Modulation of MMP1 expression by *SMARCD1* siRNA transfection

To confirm that the MMP1 expression is regulated by *SMARCD1*, we investigated the expression levels of MMP1 mRNA after *SMARCD1* siRNA transfection. As shown in Fig. 4a, *SMARCD1* mRNA expression was significantly suppressed by *SMARCD1* siRNA transfection ($p < 0.005$). As shown in Fig. 4b, the expression levels of *MMP1* mRNA was significantly upregulated by *SMARCD1* siRNA transfection ($p < 0.05$).

Cell motility

As shown in Fig. 5a and b, the transwell invasion assay revealed that the number of invaded cells was significantly increased by hsa-miR-100-5p transfection ($p < 0.05$).

We also investigated the effects of hsa-miR-100-5p on the motility of NESC by an in vitro wound healing assay. As shown in Fig. 5c and d, the repaired area was significantly increased by hsa-miR-100-5p transfection ($p < 0.0005$).

Discussion

To understand the role of hsa-miR-100-5p, which is up-regulated in ECSCs, in the pathogenesis of

endometriosis, we evaluated its expression in both ECSCs and NESC. We also evaluated the hsa-miR-100-5p-mediated effects on the cellular functions of NESC and sought to determine the underlying mechanisms of hsa-miR-100-5p action in those cells. With the present study, we found the following: (1) Expression of hsa-miR-100-5p in ECSCs was upregulated compared to that in NESC. (2) hsa-miR-100-5p transfection enhanced the motility of NESC. (3) hsa-miR-100-5p promoted these cellular functions through downregulation of *SMARCD1* mRNA and induction of MMP1 expression. This suggests that hsa-miR-100-5p overexpression induces NESC to acquire the highly motile characteristics of endometriosis and is involved in promoting the development and progression of this disease.

hsa-miR-100-5p can act as either a tumor suppressor gene or an oncogene, depending on the tumor type in different cancers [19, 20]. For example, hsa-miR-100-5p overexpression has been demonstrated in nasopharyngeal cancer [21], esophageal squamous cell carcinoma [22], colon cancer [19, 23], and gastric cancer [24]. In these tumors, this miRNA contributes to tumor progression. In contrast, hsa-miR-100-5p expression is suppressed in epithelial ovarian cancer [25], endometrial cancer [26], bladder carcinoma [27], renal cell carcinoma

Table 1 List of mRNAs aberrantly expressed in miR-100-5p-transfected NESC

Gene family	Gene symbol	Control signal	miR-100 precursor signal	Z-score	Ratio	
(A) Upregulated mRNAs						
Cytokine	<i>CCL2</i>	312.22	1041.65	6.87	4.32	
	<i>IL11</i>	1034.43	2782.35	5.98	3.11	
	<i>LIF</i>	128.77	261.89	3.80	2.46	
	<i>RP2</i>	838.00	1737.49	4.13	2.17	
Growth factor	<i>BMP2</i>	817.37	461.26	-4.41	0.45	
Peptidase	<i>MMP1</i>	49,499.07	74,041.18	7.47	2.40	
	<i>CPXM1</i>	70.96	120.43	2.27	2.40	
Enzyme	<i>ASPH</i>	1259.03	3722.52	6.99	3.81	
	<i>CYBRD1</i>	1067.64	1867.57.94	4.18	2.08	
	<i>MTAP</i>	440.73	714.19	3.88	2.18	
Transcription regulator	<i>UBE2V1</i>	2487.25	6026.87	5.85	2.87	
	<i>SCML1</i>	48.29	98.99	3.02	2.53	
	<i>BATF3</i>	147.71	291.50	3.05	2.02	
Transmembrane receptor	<i>ITGA6</i>	1383.58	2680.82	4.48	2.21	
	<i>PVRL2</i>	6699.21	13,211.87	4.72	2.04	
Transporter	<i>ABCA1</i>	134.70	270.47	3.29	2.12	
	<i>BCAP29</i>	1166.81	1994.48	4.09	2.03	
Other	<i>TUBB2B</i>	41.72	123.42	4.64	3.54	
	<i>PKIA</i>	192.01	593.66	5.84	3.20	
	<i>PALM3</i>	260.83	736.98	5.72	2.99	
	<i>CEND1</i>	196.72	412.79	4.30	2.80	
	<i>EMC10</i>	4713.79	9455.68	5.88	2.76	
	<i>ERLIN2</i>	225.65	451.23	3.82	2.41	
	<i>TFPI2</i>	752.91	1839.06	4.64	2.35	
	<i>RDX</i>	469.66	816.51	4.11	2.27	
	<i>FAM131B</i>	47.52	91.03	2.61	2.24	
	<i>SWAP70</i>	440.11	805.17	4.01	2.18	
	<i>LOC728392</i>	1643.31	3433.27	4.56	2.15	
	<i>STBD1</i>	104.93	162.95	3.20	2.15	
	<i>SNRPC</i>	10,269.42	17,744.24	4.89	2.12	
	Other	<i>CIDEA</i>	488.37	852.48	3.68	2.05
		<i>ANGPTL4</i>	1403.18	2829.40	4.28	2.01
Null	<i>LOC102723946</i>	38.79	110.21	3.88	3.33	
(B) Downregulated mRNAs						
Enzyme	<i>HSD17B2</i>	286.50	128.94	-5.76	0.26	
	<i>PLCH1</i>	190.28	88.66	-4.24	0.38	
	<i>INMT</i>	1404.19	713.49	-5.10	0.40	
Ion channel	<i>KCNN2</i>	118.10	32.10	-4.34	0.24	
	<i>KCTD4</i>	151.44	53.14	-5.41	0.28	
	<i>KCTD10</i>	1074.65	563.34	-4.14	0.47	
Kinase	<i>FGFR3</i>	239.75	121.71	-3.31	0.49	
Peptidase	<i>ADAMTSS</i>	3143.19	1023.39	-6.74	0.33	
	<i>ADAM19</i>	239.21	117.14	-3.26	0.47	

Table 1 List of mRNAs aberrantly expressed in miR-100-5p-transfected NESCs (*Continued*)

Gene family	Gene symbol	Control signal	miR-100 precursor signal	Z-score	Ratio
Phosphatase	<i>LPPR4</i>	184.80	73.50	-4.33	0.34
Transcription regulator	<i>SMARCD1</i>	2210.80	932.50	-5.34	0.43
	<i>BAZ2A</i>	288.00	135.67	-3.32	0.47
Transporter	<i>ATP6AP1</i>	9337.60	3682.26	-6.29	0.40
Other	<i>EPDR1</i>	3173.94	780.35	-8.19	0.27
	<i>MPZL3</i>	125.86	59.79	-3.82	0.43
	<i>ZBED2</i>	161.28	71.97	-3.74	0.43
	<i>SUDS3</i>	568.38	289.31	-4.34	0.46
	<i>CGA</i>	112.70	61.15	-3.01	0.46
	<i>TMEM30A</i>	3229.37	1492.02	-4.80	0.47
	<i>DGCR2</i>	4328.05	2074.04	-4.65	0.47
	<i>CTDSPL</i>	748.62	362.73	-4.11	0.48
	<i>DEPTOR</i>	398.87	187.27	-3.37	0.48
	<i>DNAJC11</i>	1560.93	839.74	-3.46	0.49
	<i>CLDN11</i>	1351.65	687.71	-3.46	0.49
Null	<i>SLC16A14</i>	144.45	54.61	-3.92	0.35
	<i>PROSER2-AS1</i>	35.66	16.12	-2.11	0.42
	<i>AREG</i>	120.26	61.28	-3.53	0.43

ABCA1 ATP-binding cassette, sub-family A, member 1; *ADAM19* ADAM metalloproteinase domain 19; *ADAMTS5* ADAM metalloproteinase with thrombospondin type 1 motif, 5; *ANGPTL4* angiopoietin-like 4 transcript variant 1; *AREG* amphiregulin; *ASPH* aspartate beta-hydroxylase, transcript variant 3; *ATP6AP1* ATPase, H⁺ transporting, lysosomal accessory protein 1; *BATF3* basic leucine zipper transcription factor, ATF-like 3; *BAZ2A* bromodomain adjacent to zinc finger domain, 2A; *BCAP29* B-cell receptor-associated protein 29, transcript variant 2; *BMP2* bone morphogenetic protein 2; *CCL2* chemokine ligand 2; *CEND1* cell cycle exit and neuronal differentiation 1; *CGA* glycoprotein hormones, alpha polypeptide, transcript variant 2; *CIDEA* cell death-inducing DFFA-like effector c, transcript variant 3; *CLDN11* claudin 11, transcript variant 1; *CPXM1* carboxypeptidase X, member 1, transcript variant 1; *CTDSPL* CTD (carboxy-terminal domain, RNA polymerase II, polypeptide A) small phosphatase-like, transcript variant 1; *CYBRD1* cytochrome b reductase 1, transcript variant 1; *DEPTOR* DEP domain containing MTOR-interacting protein, transcript variant 1; *DGCR2* DiGeorge syndrome critical region gene 2, transcript variant 1; *DNAJC11* DnaJ (Hsp40) homolog, subfamily C, member 11; *EMC10* ER membrane protein complex subunit 10, transcript variant 1; *EPDR1* ependymin related 1, transcript variant 1; *ERLIN2* ER lipid raft associated 2, transcript variant 1; *FAM131B* family with sequence similarity 131, member B, transcript variant a; *FGFR3* fibroblast growth factor receptor 3, transcript variant 1; *HSD17B2* hydroxysteroid (17-beta) dehydrogenase 2; *IL11* interleukin 11; *INMT* indolethylamine N-methyltransferase, transcript variant 2; *ITGA6* integrin, alpha 6, transcript variant 2; *KCNK2* potassium channel, calcium activated intermediate/small conductance subfamily N alpha, member 2, transcript variant 1; *KCTD10* potassium channel tetramerization domain containing 10; *KCTD4* potassium channel tetramerization domain containing 4; *LIF* leukemia inhibitory factor, transcript variant 1; *LOC102723946*, Zinc finger protein 695; *LOC728392*, uncharacterized *LOC728392*; *LPPR4* lipid phosphate phosphatase-related protein type 4, transcript variant 1; *MMP1* matrix metalloproteinase 1, transcript variant 1; *MPZL3* myelin protein zero-like 3, transcript variant 1; *MTAP* methylthioadenosine phosphorylase; *PALM3* paralemm 3; *PKIA* protein kinase (cAMP-dependent, catalytic) inhibitor alpha, transcript variant 1; *PLCH1* phospholipase C, eta 1, transcript variant 2; *PROSER2-AS1* PROSER2 antisense RNA 1; *PVRL2* poliovirus receptor-related 2, transcript variant delta; *RDX* radixin, transcript variant 3; *RP2* retinitis pigmentosa 2; *SCML1* sex comb on midleg-like 1, transcript variant 1; *SLC16A14* solute carrier family 16, member 14; *SMARCD1* SWI/SNF related, matrix associated, actin dependent regulator of chromatin, subfamily d, member 1, transcript variant 2; *SNRPC* small nuclear ribonucleoprotein polypeptide C, transcript variant 1; *STBD1* starch binding domain 1; *SUDS3* suppressor of defective silencing 3 homolog; *SWAP70* SWAP switching B-cell complex 70 kDa subunit, transcript variant 1; *TFPI2* tissue factor pathway inhibitor 2, transcript variant 1; *TMEM30A* transmembrane protein 30A, transcript variant 1; *TUBB2B* tubulin, beta 2B class IIb; *UBE2V1* ubiquitin-conjugating enzyme E2 variant 1, transcript variant 4; *ZBED2* zinc finger, BED-type containing 2

[28], prostate cancer [29], breast carcinoma [30], hepatocellular carcinoma [31], and non-small cell lung cancer [32]. In these tumors, this miRNA behaves as a tumor suppressor.

The reported target genes of hsa-miR-100-5p include polo-like kinase 1 [21, 32], insulin-like growth factor (IGF) [33], IGF-1 receptor [34], mammalian target of rapamycin (mTOR) [34], fibroblast growth factor receptor 3 [35], ataxia telangiectasia mutated (ATM) [36], Argonaute 2 [37], isoprenylcysteine carboxyl methyltransferase (ICMT) [38], nuclear factor- κ B3 [39], ras-related C3 botulinum toxin substrate 1 (Rac1) [38], and β -tubulin [40].

To our knowledge, there is no report which evaluated the expression and function of *SMARCD1* in endometriosis. Whereas, overexpression of *MMP1* is reported in endometriotic tissues [14], however, the roles of *MMP1* regarding the pathogenesis of endometriosis has not been elucidated yet. *MMP1* gene polymorphisms may also affect the motility of ECSCs [13]. In the present study, we demonstrated that transfection with hsa-miR-100-5p induced *MMP1* expression in NESCs through downregulation of *SMARCD1* and that *MMP1* accelerated the migration of NESCs.

A limitation of the present study is that the experiments were performed only with the stromal cells of

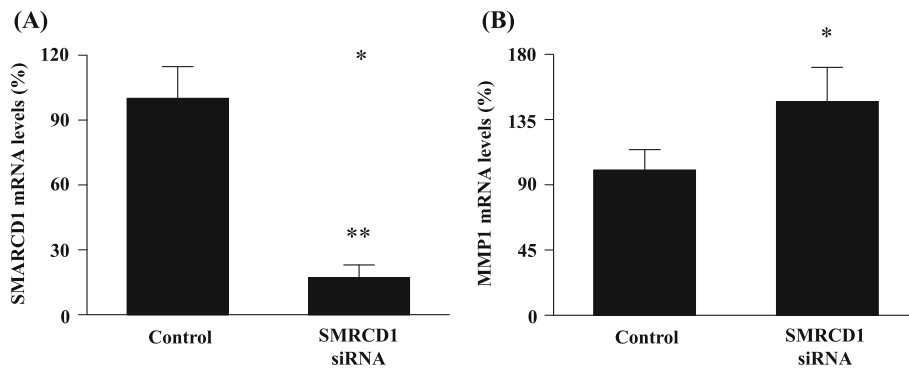


Fig. 4 Effects of SMARCD1 siRNA transfection on the MMP1 mRNA expression in NESC. **(a)** SMARCD1 mRNA expression after SMARCD1 siRNA transfection. **(b)** MMP1 mRNA expression. * $p < 0.05$, ** $p < 0.005$ vs. controls (Student's *t*-test). MMP1, matrix metalloproteinase 1; NESC, normal endometrial stromal cells; SMARCD1, SWItch/sucrose non-fermentable-related matrix-associated actin-dependent regulator of chromatin subfamily D member 1

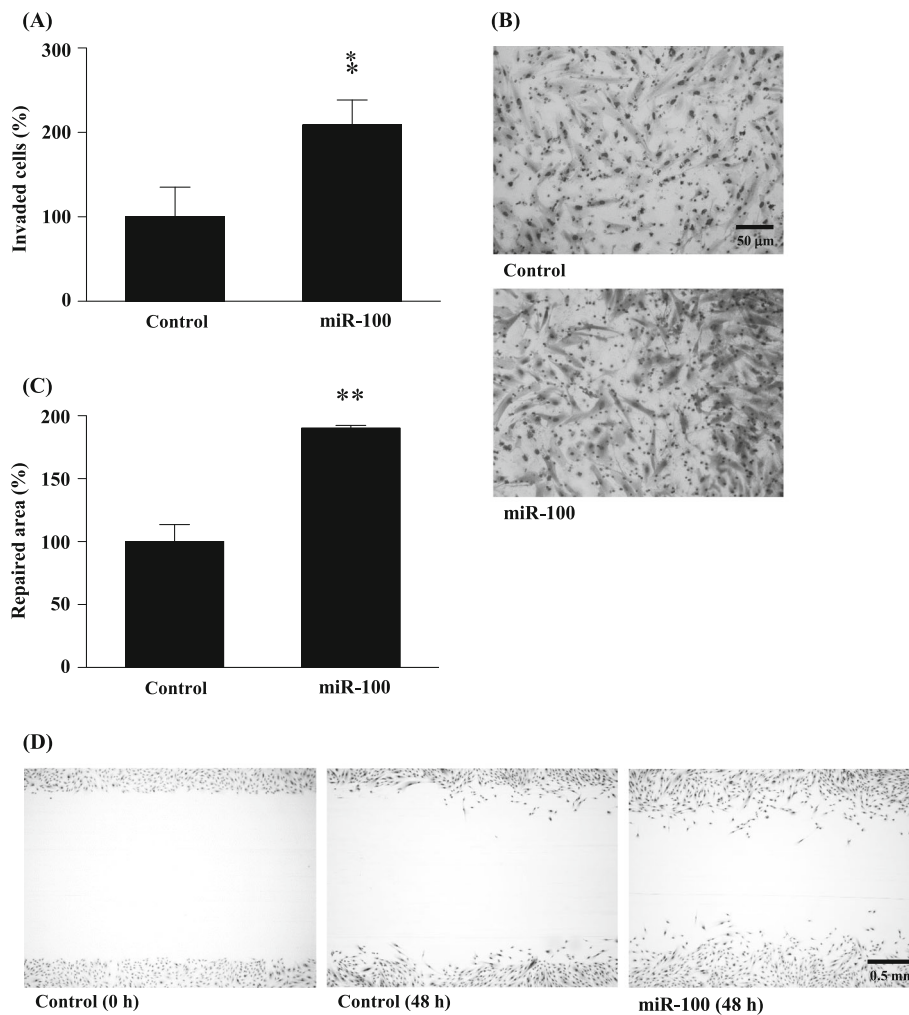


Fig. 5 Effects of hsa-miR-100-5p transfection on the motility of NESC. **(a)** Results of transwell invasion assay. **(b)** Representative photographs of transwell invasion assay. **(c)** Results of in-vitro wound repair assay. **(d)** Representative photographs of in vitro wound repair assay. * $p < 0.05$, ** $p < 0.0005$ vs. controls (Student's *t*-test). NESC, normal endometrial stromal cells

endometriosis and the eutopic endometrium of women without endometriosis. Due to difficulties in obtaining samples, the expression of hsa-miR-100-5p in the eutopic endometrium of women with endometriosis was not evaluated. Future study is necessary on this point.

Conclusions

In summary, we confirmed that hsa-miR-100-5p expression is upregulated in ECSCs. By transfecting hsa-miR-100-5p into NESCs, we observed that SMARCD1/MMP-1 is the downstream pathway of hsa-miR-100-5p. Inhibition of SMARCD1 mRNA expression, followed by MMP1 activation, enhanced the motility of NESCs. These findings suggest that enhanced expression of hsa-miR-100-5p in endometriosis is involved a role in promoting the acquisition of endometriosis-specific characteristics during the development of endometriosis. Our present findings on the roles of hsa-miR-100-5p may thus contribute to understand the epigenetic mechanisms involved in the pathogenesis of endometriosis.

Abbreviations

ATM: Ataxia telangiectasia mutated; DMEM: Dulbecco's modified Eagle medium; ECSCs: Endometriotic cyst stromal cells; ELISA: Enzyme-linked immunosorbent assay; FBS: Fetal bovine serum; GAPDH: Glyceraldehyde 3-phosphate dehydrogenase; ICMT: Isoprenylcysteine carboxyl methyltransferase; IGF: Insulin-like growth factor; IPA: Ingenuity pathways analysis; IRB: Institutional Review Board; miRNA: microRNA; MMP1: Matrix metalloproteinase 1; mTOR: Mammalian target of rapamycin; NESCs: Normal endometrial stromal cells; Rac1: Ras-related C3 botulinum toxin substrate 1; RT-PCR: Reverse transcription-polymerase chain reaction; siRNA: Small interfering RNA; SMARCD1: SWI/SNF-related matrix-associated actin-dependent regulator of chromatin subfamily D member 1; SWI/SNF: SWI/SNF sucrose non-fermentable

Acknowledgements

We would like to thank Ms. Sawako Adachi and Ms. Nozomi Kai for their excellent technical assistance and Editage (www.editage.jp) for English language editing.

Authors' contributions

KN participated in the study design, data analysis and interpretation, literature search, generation of figures, and writing and editing the manuscript. KT, MO, YA, TH and HN executed the data/case collection, experiments, data analysis, and interpretation. All authors read and approved the final manuscript.

Funding

This work was supported in part by Grants-in-Aid for Scientific Research from the Japan Society for the Promotion of Science (no. 16 K11093 to K. Nasu, no. 18 K16774 to T. Hirakawa, no. 17 K16857 to K. Takebayashi, and no. 15 K10679 to H. Narahara) and the Study Fund of Oita Society of Obstetrics and Gynecology (to T. Hirakawa and Y. Aoyagi).

Availability of data and materials

All the gene expression microarray data are available at the Gene Expression Omnibus through the NCBI under Accession No. GSE139954 (<https://www.ncbi.nlm.nih.gov/geo/query/acc.cgi?acc=GSE139954>). Other data in this study are available from the corresponding author.

Ethics approval and consent to participate

The present study was approved by the Institutional Review Board (IRB) of the Faculty of Medicine, Oita University (registration number: P-16-01). Written informed consent was obtained from all the patients.

Consent for publication

Not applicable.

Competing interests

There are no conflicts of interest to declare.

Received: 3 January 2020 Accepted: 13 April 2020

Published online: 16 April 2020

References

- Giudice LC. Clinical practice. Endometriosis *N Engl J Med*. 2010;362:2389–98.
- Nasu K, Yuge A, Tsuno A, Narahara H. Mevalonate-Ras homology (rho)/rho-associated coiled-coil-forming protein kinase (ROCK)-mediated signaling pathway as a therapeutic target for the treatment of endometriosis-associated fibrosis. *Curr Signal Transduct Ther*. 2010;5:141–8.
- Nasu K, Nishida M, Kawano Y, Tsuno A, Abe W, Yuge A, Takai N, Narahara H. Aberrant expression of apoptosis-related molecules in endometriosis: a possible mechanism underlying the pathogenesis of endometriosis. *Reprod Sci*. 2011;18:206–18.
- Abe W, Nasu K, Nakada C, Kawano Y, Moriyama M, Narahara H. miR-196b targets c-Myc and Bcl-2 expression, inhibits proliferation and induces apoptosis in endometriotic stromal cells. *Hum Reprod*. 2013;28:750–61.
- Okamoto M, Nasu K, Abe W, Aoyagi Y, Kawano Y, Kai K, Moriyama M, Narahara H. Enhanced miR-210 expression promotes the pathogenesis of endometriosis through activation of signal transducer and activator of transcription 3. *Hum Reprod*. 2015;30:632–41.
- Hirakawa T, Nasu K, Abe W, Aoyagi Y, Okamoto M, Kai K, Takebayashi K, Narahara H. miR-503, a microRNA epigenetically repressed in endometriosis, induces apoptosis and cell-cycle arrest and inhibits cell proliferation, angiogenesis, and contractility of human ovarian endometriotic stromal cells. *Hum Reprod*. 2016;31:2587–97.
- Aoyagi Y, Nasu K, Kai K, Hirakawa T, Okamoto M, Kawano Y, Abe W, Tsukamoto Y, Moriyama M, Narahara H. Decidualization differentially regulates microRNA expression in eutopic and ectopic endometrial stromal cells. *Reprod Sci*. 2017;24:445–55.
- Zhang P, Li L, Bao Z, Huang F. Role of BAF60a/BAF60c in chromatin remodeling and hepatic lipid metabolism. *Nutr Metab*. 2016;13:30.
- Arts FA, Keogh L, Smyth P, O'Toole S, Ta R, Gleeson N, O'Leary JJ, Flavin R, Sheils O. miR-223 potentially targets SWI/SNF complex protein SMARCD1 in atypical proliferative serous tumor and high-grade ovarian serous carcinoma. *Hum Pathol*. 2017;70:98–104.
- Ring HZ, Vameghi-Meyers V, Wang W, Crabtree GR, Francke U. Five SWI/SNF-related, matrix-associated, actin-dependent regulator of chromatin (SMAR) genes are dispersed in the human genome. *Genomics*. 1998;51:140–3.
- Bultman S, Gebuhr T, Yee D, La Mantia C, Nicholson J, Gilliam A, Randazzo F, Metzger D, Chambon P, Crabtree G, Magnuson T. A Brg1 null mutation in the mouse reveals functional differences among mammalian SWI/SNF complexes. *Mol Cell*. 2000;6:1287–95.
- Roberts CW, Orkin SH. The SWI/SNF complex—chromatin and cancer. *Nat Rev Cancer*. 2004;4:133–42.
- Arakaki PA, Marques MR, Santos MCLG. MMP-1 polymorphism and its relationship to pathological processes. *J Biosci*. 2009;34:313–20.
- Kokorine I, Nisolle M, Donnez J, Eeckhout Y, Courtoy PJ, Marbaix E. Expression of interstitial collagenase (matrix metalloproteinase-1) is related to the activity of human endometriotic lesions. *Fertil Steril*. 1997;68:246–51.
- Nishida M, Nasu K, Fukuda J, Kawano Y, Narahara H, Miyakawa I. Down regulation of interleukin-1 receptor expression causes the dysregulated expression of CXC chemokines in endometriotic stromal cells: a possible mechanism for the altered immunological functions in endometriosis. *J Clin Endocrinol Metab*. 2004;89:5094–100.
- Matsumoto H, Nasu K, Nishida M, Ito H, Bing S, Miyakawa I. Regulation of proliferation, motility, and contractility of human endometrial stromal cells by platelet-derived growth factor. *J Clin Endocrinol Metab*. 2005;90:3560–7.
- Nasu K, Nishida M, Matsumoto H, Sun B, Inoue C, Kawano Y, Miyakawa I. Regulation of proliferation, motility, and contractility of cultured human endometrial stromal cells by transforming growth factor-beta isoforms. *Fertil Steril*. 2005;84(Suppl):1114–23.
- Hendricks KB, Shanahan F, Lees E. Role for BRG1 in cell cycle control and tumor suppression. *Mol Cell Biol*. 2004;24:362–76.

19. Chen P, Xi Q, Wang Q, Wei P. Downregulation of microRNA-100 correlates with tumor progression and poor prognosis in colorectal cancer. *Med Oncol*. 2014;31:235.
20. Wang H, Wang L, Wu Z, Sun R, Jin H, Ma J, Liu L, Ling R, Yi J, Wang L, Bian J, Chen J, Li N, Yuan S, Yun J. Three dysregulated microRNAs in serum as novel biomarkers for gastric cancer screening. *Med Oncol*. 2014;31:298.
21. Shi W, Alajez NM, Bastianutto C, Hui AB, Mocanu JD, Ito E, Busson P, Lo KW, Ng R, Waldron J, O'Sullivan B, Liu FF. Significance of Plk1 regulation by miR-100 in human nasopharyngeal cancer. *Int J Cancer*. 2010;126:2036–48.
22. Ko MA, Zehong G, Virtanen C, Guindi M, Waddell TK, Keshavjee S, Darling GE. MicroRNA expression profiling of esophageal cancer before and after induction chemoradiotherapy. *Ann Thorac Surg*. 2012;94:1094–102.
23. Rokavec M, Horst D, Hermeking H. Cellular model of colon cancer progression reveals signatures of mRNAs, miRNA, lncRNAs, and epigenetic modifications associated with metastasis. *Cancer Res*. 2017;77:1854–67.
24. Shi D-B, Wang Y-W, Xing A-Y, Gao J-W, Zhang H, Guo X-Y, Gao P. C/EBP α -induced miR-100 expression suppresses tumor metastasis and growth by targeting ZBTB7A in gastric cancer. *Cancer Lett*. 2015;369:376–85.
25. Peng DX, Luo M, Qiu LW, He YL, Wang XF. Prognostic implications of microRNA-100 and its functional roles in human epithelial ovarian cancer. *Oncol Rep*. 2012;27:1238–44.
26. Torres A, Torres K, Pesci A, Ceccaroni M, Paszkowski T, Cassandrini P, Zamboni G, Maciejewski R. Deregulation of miR-100, miR-99a and miR-199b in tissues and plasma coexists with increased expression of mTOR kinase in endometrioid endometrial carcinoma. *BMC Cancer*. 2012;12:369.
27. Wang S, Xue S, Dai Y, Yang J, Chen Z, Fang X, Zhou W, Wu W, Li Q. Reduced expression of microRNA-100 confers unfavorable prognosis in patients with bladder cancer. *Diagn Pathol*. 2012;7:159.
28. Wang G, Chen L, Meng J, Chen M, Zhuang L, Zhang L. Overexpression of microRNA-100 predicts an unfavorable prognosis in renal cell carcinoma. *Int Urol Nephrol*. 2013;45:373–9.
29. Leite KR, Tomiyama A, Reis ST, Sousa-Canavez JM, Sanudo A, Camara-Lopes LH, Srougi M. MicroRNA expression profiles in the progression of prostate cancer from high-grade prostate intraepithelial neoplasia to metastasis. *Urol Oncol*. 2013;31:796–801.
30. Gebeshuber CA, Martinez J. miR-100 suppresses IGF2 and inhibits breast tumorigenesis by interfering with proliferation and survival signaling. *Oncogene*. 2013;32:3306–10.
31. Chen P, Zhao X, Ma L. Downregulation of microRNA-100 correlates with tumor progression and poor prognosis in hepatocellular carcinoma. *Mol Cell Biochem*. 2013;383:49–58.
32. Liu J, Lu KH, Liu ZL, Sun M, De W, Wang ZX. MicroRNA-100 is a potential molecular marker of non-small cell lung cancer and functions as a tumor suppressor by targeting polo-like kinase 1. *BMC Cancer*. 2012;12:519.
33. Tovar V, Alsinet C, Villanueva A, Hoshida Y, Chiang DY, Solé M, Thung S, Moyano S, Toffanin S, Minguez B, Cabellos L, Peix J, Schwartz M, Mazzaferro V, Bruix J, Llovet JM. IGF activation in a molecular subclass of hepatocellular carcinoma and pre-clinical efficacy of IGF-1R blockage. *J Hepatol*. 2010;52:550–9.
34. Ge YY, Shi Q, Zheng ZY, Gong J, Zeng C, Yang J, Zhuang SM. MicroRNA-100 promotes the autophagy of hepatocellular carcinoma cells by inhibiting the expression of mTOR and IGF-1R. *Oncotarget*. 2014;5:6218–28.
35. Luan Y, Zhang S, Zuo L, Zhou L. Overexpression of miR-100 inhibits cell proliferation, migration, and chemosensitivity in human glioblastoma through FGFR3. *Onco Targets Ther*. 2015;8:3391–400.
36. Ng WL, Yan D, Zhang X, Mo YY, Wang Y. Over-expression of miR-100 is responsible for the low-expression of ATM in the human glioma cell line: M059J. *DNA Repair*. 2010;9:1170–5.
37. Wang M, Ren D, Guo W, Wang Z, Huang S, Du H, Song L, Peng X. Loss of miR-100 enhances migration, invasion, epithelial-mesenchymal transition and stemness properties in prostate cancer cells through targeting Argonaute 2. *Int J Oncol*. 2014;45:362–72.
38. Zhou HC, Fang JH, Luo X, Zhang L, Yang J, Zhang C, Zhuang SM. Downregulation of microRNA-100 enhances the ICMT-Rac1 signaling and promotes metastasis of hepatocellular carcinoma cells. *Oncotarget*. 2014;5:12177–88.
39. Liu M, Han T, Shi S, Chen E. Long noncoding RNA HAGLROS regulates cell apoptosis and autophagy in lipopolysaccharides-induced WI-38 cells via modulating miR-100/NF- κ B axis. *Biochem Biophys Res Commun*. 2018;500:589–96.
40. Lobert S, Jefferson B, Morris K. Regulation of β -tubulin isotypes by microRNA 100 in MCF7 breast cancer cells. *Cytoskeleton*. 2011;68:355–62.

Publisher's Note

Springer Nature remains neutral with regard to jurisdictional claims in published maps and institutional affiliations.

Ready to submit your research? Choose BMC and benefit from:

- fast, convenient online submission
- thorough peer review by experienced researchers in your field
- rapid publication on acceptance
- support for research data, including large and complex data types
- gold Open Access which fosters wider collaboration and increased citations
- maximum visibility for your research: over 100M website views per year

At BMC, research is always in progress.

Learn more [biomedcentral.com/submissions](https://www.biomedcentral.com/submissions)

